AGU PUBLICATIONS

Geophysical Research Letters

RESEARCH LETTER
10.1002/2016GL068734

Key Points:
- Preindustrial AoA variations are small in comparison to the changes of the 20th and 21st centuries
- Strong volcanic eruptions cause the largest change in AoA on a time scale of several years
- The solar influence is small and differs for UV and non-UV variations

Supporting Information:
- Supporting Information S1

Correspondence to:
S. Muthers,
muthers@climate.unibe.ch

Citation:
Muthers, S., A. Kuchar, A. Stenke, J. Schmitt, J. G. Anet, C. C. Raible, and T. F. Stocker (2016), Stratospheric age of air variations between 1600 and 2100, *Geophys. Res. Lett.*, *43*, doi:10.1002/2016GL068734.

Received 18 FEB 2016
Accepted 14 APR 2016
Accepted article online 30 APR 2016

Stratospheric age of air variations between 1600 and 2100

S. Muthers[1,2], A. Kuchar[3,4], A. Stenke[3], J. Schmitt[1,2], J. G. Anet[5], C. C. Raible[1,2], and T. F. Stocker[1,2]

[1]Climate and Environmental Physics, University of Bern, Bern, Switzerland, [2]Oeschger Centre for Climate Change Research, University of Bern, Bern, Switzerland, [3]Institute for Atmospheric and Climate Science, ETH Zurich, Zurich, Switzerland, [4]Department of Atmospheric Physics, Faculty of Mathematics and Physics, Charles University in Prague, Prague, Czech Republic, [5]Swiss Federal Laboratories for Material Science and Technology (Empa), Dübendorf, Switzerland

Abstract The current understanding of preindustrial stratospheric age of air (AoA), its variability, and the potential natural forcing imprint on AoA is very limited. Here we assess the influence of natural and anthropogenic forcings on AoA using ensemble simulations for the period 1600 to 2100 and sensitivity simulations for different forcings. The results show that from 1900 to 2100, CO_2 and ozone-depleting substances are the dominant drivers of AoA variability. With respect to natural forcings, volcanic eruptions cause the largest AoA variations on time scales of several years, reducing the age in the middle and upper stratosphere and increasing the age below. The effect of the solar forcing on AoA is small and dominated by multidecadal total solar irradiance variations, which correlate negatively with AoA. Additionally, a very weak positive relationship driven by ultraviolett variations is found, which is dominant for the 11 year cycle of solar variability.

1. Introduction

The mean Age of Air (AoA) describes the transport time along the Brewer-Dobson circulation (BDC) [*Hall and Plumb*, 1994; *Waugh and Hall*, 2002], and changes in AoA are therefore a proxy for changes in the strength of the BDC [*Austin and Li*, 2006]. This meridional circulation in the stratosphere shows rising motion in the tropics and downward transport in the middle and high latitudes [*Holton et al.*, 1995; *Butchart*, 2014] and is driven by atmospheric waves [e.g., *Plumb*, 2002]. Besides the transport through the residual circulation, AoA is also a function of eddy mixing [*Ploeger et al.*, 2014, 2015]. Horizontal mixing between the tropics and extratropics, for instance, can increase the overall age of the stratospheric air by recirculating aged air from the midlatitudes into the tropical pipe—a process which is called *aging by mixing* [*Garny et al.*, 2014]. A stratospheric air parcel therefore consists of different ages—expressed by an age distribution—where the mean AoA is the first moment of this distribution. This value cannot be measured directly but is calculated from measurements of (long-lived) atmospheric gases, like sulfur hexafluoride (SF_6) or carbon dioxide (CO_2) [e.g., *Stiller et al.*, 2008; *Engel et al.*, 2009]. Under the assumption that tropospheric trace gas concentrations increase or decrease continuously, the age of a certain stratospheric air parcel is given by the time lag between concentrations in this parcel and the troposphere.

In atmospheric general circulation models (GCMs) or chemistry-climate models (CCMs), AoA variations can be quantified by implementing a passive tracer. Previous modeling studies found a reduction of the AoA and an intensification of the tropical upward mass flux since the preindustrial era in particular since 1970 [*Butchart et al.*, 2006; *Austin et al.*, 2007, 2013; *Li et al.*, 2008]. An increase in the tropical upward mass flux is commonly interpreted as an intensification of the BDC. This change is associated with the tropospheric warming and stratospheric cooling caused by rising concentrations of greenhouse gases (GHGs) and stratospheric ozone depletion. The relative contributions of these different forcing factors, however, depend on altitude. In particular, ozone-depleting substances (ODS) can lead to a local increase in AoA [*Oberländer-Hayn et al.*, 2015]. For the future, model simulations project a further intensification of the BDC and reduction of AoA under rising GHG concentrations [*Butchart and Scaife*, 2001; *Butchart et al.*, 2010; *Garcia and Randel*, 2008; *Li et al.*, 2008; *Bunzel and Schmidt*, 2013]. The projected recovery of stratospheric ozone slightly counteracts theses trends, but future changes of AoA are dominated by the CO_2 effect [*Shepherd and Jonsson*, 2008; *Oberländer et al.*, 2013].

While the simulated results for the last decades of the twentieth century draw a very consistent picture of AoA and BDC changes, no agreement is found in observation-based studies. The results of these studies range

from a slight increase [e.g., *Engel et al.*, 2009] (based on SF_6 and CO_2 measurements from high-altitude balloon flights for the period 1975–2005) to a clear reduction of AoA [e.g., *Remsberg*, 2015] (using CH_4 records for the period 1995–2005). These AoA observations, however, are based on spatially and temporally sparse observations and are therefore associated with large uncertainties [*Waugh*, 2009; *Garcia et al.*, 2011]. *Engel et al.* [2009] for instance used the data of 27 balloon flights from the midlatitudes of the Northern Hemisphere (NH) for their trend analysis over a 30 year period. Furthermore, using nonuniformly increasing trace gases for AoA estimates is suggested to underestimate AoA trends [*Garcia et al.*, 2011]. AoA and BDC changes estimated from reanalysis data sets agree fairly well with CCM results [*Abalos et al.*, 2015; *Fu et al.*, 2015].

Strong volcanic eruptions inject large amounts of sulfur compounds into the atmosphere, which are transformed to sulfate aerosols in the stratosphere. These aerosols absorb infrared radiation and have a strong effect on the stratospheric dynamics and therefore on AoA and the BDC. In climate models, an intensification of the BDC after volcanic eruptions has been reported in many studies [*Pitari*, 1993; *Pitari and Mancini*, 2002; *Garcia et al.*, 2011; *Aquila et al.*, 2013; *Toohey et al.*, 2014]. These results are supported by observations. Using reanalysis products, *Graf et al.* [2007] found enhanced wave activity in the northern winter stratosphere after the eruptions of Agung, El Chichon, and Pinatubo. Furthermore, *Schnadt Poberaj et al.* [2011] identified anomalous stratospheric wave activity and a strengthened BDC to be the reason for the relatively high ozone concentrations in the Southern Hemisphere after Pinatubo. *Abalos et al.* [2015] confirmed a strengthening of the circulation when the BDC is derived from the momentum balance equation in all modern reanalyses (i.e., Modern Era Retrospective-Analysis for Research and Applications (MERRA), ECMWF Interim Reanalysis (ERA-Interim), and Japanese 55-year Reanalysis (JRA-55)). However, *Diallo et al.* [2012] estimated an increase of AoA after Pinatubo using Lagrangian transport models with ERA-Interim reanalysis data.

Variations in the stratospheric circulation are of particular importance for the distribution of ozone in the stratosphere and the removal of ODS [*Butchart and Scaife*, 2001]. Furthermore, the distribution of different GHGs in the stratosphere depends on the stratospheric transport. Improving the current understanding of how this circulation is influenced by different forcings is crucial to predict the evolution of the stratospheric ozone concentrations in the future. Additionally, a better knowledge of possible long-term changes in AoA is of interest for the interpretation of changes in the concentration or isotopic composition of trace gas species that are predominantly destroyed in the stratosphere. Substantial changes in the stratospheric transport and thus in the residence time (lifetime) of climatic proxies may bias their interpretation. One example is the study of N_2O and its isotopic composition. N_2O is an important GHG and ozone-depleting substance. Natural emissions of N_2O are dominated by microbial activity in soils and the ocean, and changes in N_2O or its isotopic composition can be interpreted as changes in the biological activity of these sources, under the assumption of a constant atmospheric lifetime. The most important sink of N_2O is the stratospheric UV photolysis, which affects also the isotopic composition, leading to an enrichment in heavier isotopes in stratospheric N_2O and due to the stratosphere-troposphere return flux also in the troposphere [e.g., *Röckmann et al.*, 2001]. Consequently, changes in the BDC and the stratosphere-troposphere exchange rates influence the sink strength of N_2O and the associated isotope fractionation in the stratosphere and thus atmospheric lifetime and isotopic composition in the troposphere.

Up to now, AoA or BDC variations in the preindustrial era and the influence of natural forcing (e.g., solar variations or volcanic eruptions) during this period have received little attention in chemistry-climate modeling studies. *Austin et al.* [2013] simulated the period from 1860 onward using a coupled atmosphere-ocean-chemistry-climate model (AOCCM) and found little variations in AoA before 1975. However, no study has focused yet on the period before 1860, including grand solar minima such as the Dalton Minimum (1790–1830). Here we aim at assessing the influence of natural and anthropogenic forcing factors on AoA for the period 1600–2100. We rely on an ensemble of simulations using a fully coupled AOCCM and different solar forcing reconstructions and projections. The model and the experiments used in this study are described in section 2. Section 3 presents the results, in a first step (section 3.1) for the volcanic signals in AoA and in a second step (section 3.2) for the influence of the remaining forcings, i.e., solar variability, CO_2, and ODS. A discussion and summary of the results is given in section 4.

2. Model and Experimental Design

All experiments used in this study are performed with the AOCCM SOCOL-MPIOM [*Muthers et al.*, 2014]. SOCOL-MPIOM consists of SOCOL version 3 (SOlar Climate Ozone Links [*Stenke et al.*, 2013]) coupled to the

ocean-sea ice model MPIOM (Max-Plank-Institute Ocean Model [*Marsland*, 2003]). The physical modules of SOCOL are based on the middle atmospheric version of MA-ECHAM5 [*Roeckner et al.*, 2003] coupled to the chemical module MEZON (Model for Evaluation of oZONe trends [*Rozanov et al.*, 1999; *Egorova et al.*, 2003]). MA-ECHAM5 transfers temperature and tracer fields to MEZON, which calculates chemical transformations of 41 gas species participating in 200 gas phase, 16 heterogeneous, and 35 photolytic reactions. The experiments are performed with a spectral truncation of T31, corresponding to approximately 3.75° × 3.75° resolution in the horizontal dimension. In the vertical, the atmosphere is divided into 39 sigma pressure layers, from the surface up to the mesosphere at 0.01 hPa (80 km).

With the given vertical resolution SOCOL-MPIOM is not able to simulate the Quasi-Biennial Oscillation (QBO). Thus, a QBO nudging is applied [*Giorgetta et al.*, 1999] using a historical QBO reconstruction [*Brönnimann et al.*, 2007]. Note that this approach is unable to simulate any interactions between external forcings and the QBO.

In the model, AoA is implemented as a passive tracer with constant growth, injected at the surface. For each grid cell, the mean AoA is then a function of the difference between the tracer value in the grid cell and the value of the stratospheric entry region, which is set to 100 hPa at the equator. Note that AoA estimates in SOCOL are at the lower end of the range inferred from other models or observations [*SPARC*, 2010].

We use two scenarios for the period 1600–2000 forced by two different reconstructions of past solar activity using the spectral solar irradiance (SSI) reconstruction of *Shapiro et al.* [2011]. The STRONG reconstruction assumes variations corresponding to a total solar irradiance (TSI) difference of about 6 W m^{-2} between the Maunder Minimum and present day. In the MEDIUM reconstruction, the amplitude is reduced by 50% (Figure 1a). For each scenario two simulations are performed. Besides differences in solar forcing, all other forcings are the same in the four experiments (details in *Muthers et al.* [2014]). For the volcanic aerosol forcing, the reconstruction of *Arfeuille et al.* [2014] is applied.

For the future period (2000–2100) three different solar forcing scenarios have been considered, again with two model simulations for each scenario. In these experiments, GHGs follow the Representative Concentration Pathway (RCP) 4.5 scenario. In two simulations (CONST), no long-term variations of the solar forcing are considered but these simulations are forced by an artificial 11 year solar cycle. In the remaining four simulations, a future grand solar minimum is assumed, with TSI reductions of 4.2 and 6.5 W m^{-2} (MEDIUM and STRONG) averaged over the last three decades of the 21st century. Within the future period, four volcanic eruptions are prescribed (a Fuego-like eruption in 2024, a smaller eruption in 2033, an Agung-like volcanic eruption in 2060, and another smaller volcanic event in 2073). The future simulations were branched from the transient simulations in the year 2000 and are described in detail in *Anet et al.* [2013a]. Time series of the major forcings applied in the transient and future simulations are shown in Figure 1a.

Finally, an ensemble of sensitivity simulations is performed for the period 1780–1840 to assess the influence of different solar spectral intervals on the AoA during the Dalton Minimum. The short-wave radiation scheme of SOCOL includes six radiation bands, with the first interval (180–250 nm) covering the UV range. In one sensitivity experiment, the UV ensemble (DM-UV), only the radiation in these wavelengths is allowed to change in time while the remaining five intervals are kept constant using the values of the year 1780. In another experiment, the non-UV ensemble (DM-non-UV), the UV band is fixed at the year 1780 and the five non-UV bands are allowed to change in time. For comparison, a third ensemble of simulations is performed with all spectral intervals kept constant at conditions of the year 1780 (DM-REF). Each ensemble experiment consists of three simulations. The STRONG SSI reconstruction is applied in all experiments, and besides the solar forcing all other forcings (e.g., stratospheric aerosols) represent the conditions of the year 1780. Further details on the experiments can be found in *Anet et al.* [2013b]. An overview of the experiments considered in this study is given in Table S1 in the supporting information.

The aim of this study is to assess the influence of different external forcings on AoA. Therefore, we reduce the possible influence of internal variability on AoA (e.g., ENSO) by analyzing the ensemble average. The influence of volcanic aerosols on the stratosphere is limited to a few years up to a decade. On these time scales the differences between the two solar forcings applied in this study are small. For the analysis of the volcanic eruptions we therefore calculate the ensemble mean response using all experiments. To assess the influence of the solar forcing on AoA, the ensemble mean is calculated over all simulations sharing a common solar forcing (e.g., STRONG). In the following, we focus on long-term variations of AoA only and omit variations on

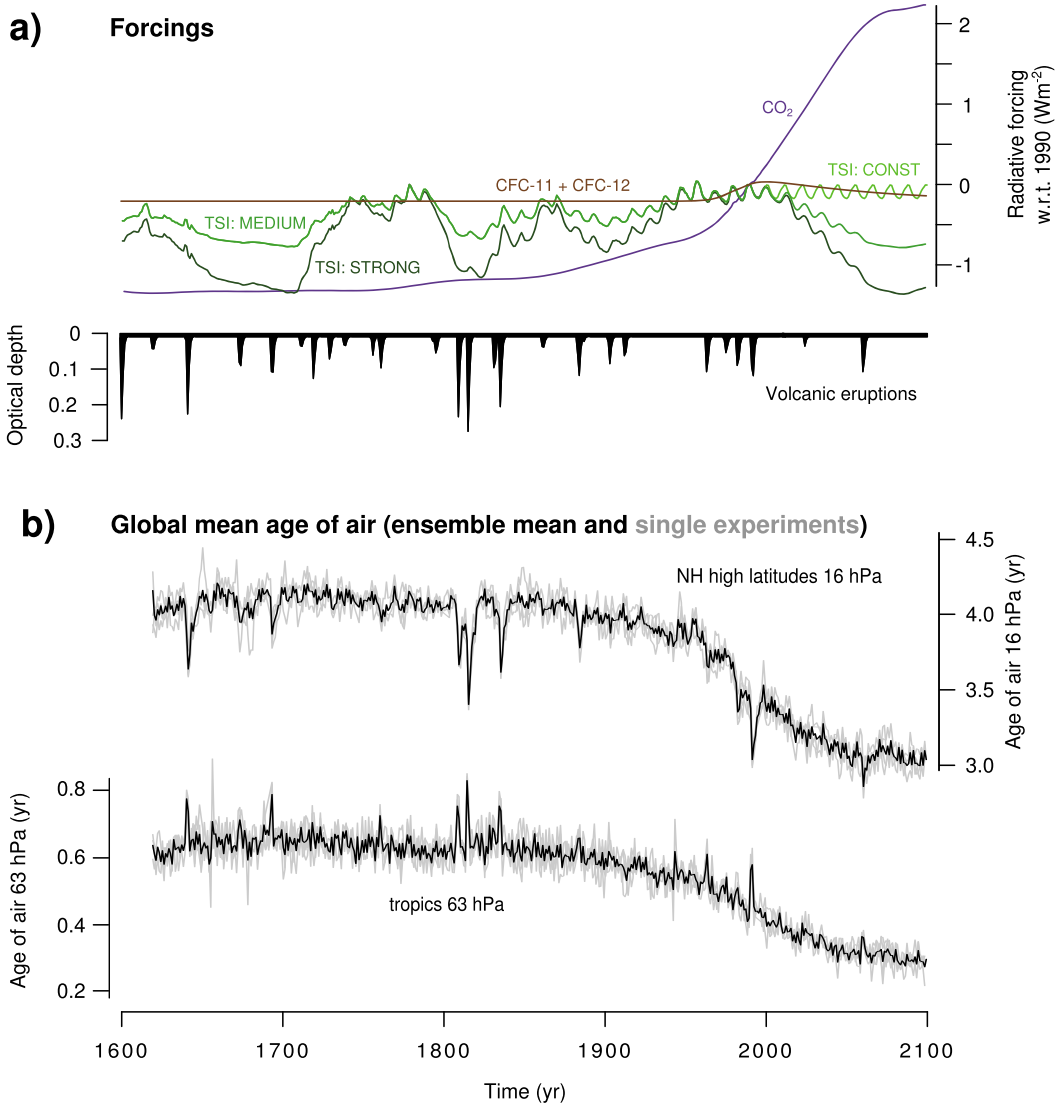

Figure 1. (a) External forcings applied in the transient simulations. For ODS (CFC-11 + CFC-12) and CO_2 the radiative forcing is given (calculated following *Ramaswamy et al.* [2001]) and TSI variations are scaled to the surface of the Earth assuming a reduction of 78% through absorption and stratospheric adjustment [*Gray et al.*, 2009]. CO_2, CFC-11, and TSI are displayed with respect to the year 1990. (b) Annual mean age of air (top) in the middle stratosphere (16 hPa) of the Northern Hemisphere high latitudes (60°N–90°N) and (bottom) in the tropical lower stratosphere (20°S to 20°N, 63 hPa). Thick black line shows the ensemble mean value of the four simulations. Thin gray lines represent the individual simulations.

the seasonal scale. Therefore, the annual mean value of AoA is used. Furthermore, to remove any influence of the spin-up phase of the model on AoA, the first 20 years from the simulations are excluded from the analysis.

3. Results

To assess the temporal changes in AoA, we focus on two specific regions. The tropical upwelling region of the BDC is represented by the mean AoA in the lower stratosphere (63 hPa) between 20°S and 20°N. The downwelling branch of the BDC in the NH high latitudes is represented by the mean AoA in the middle stratosphere (16 hPa) northward of 60°N. Note that the results below are insensitive to the definition of the regions as tests with the global average over the lower or middle stratosphere show.

Time series for both regions reveal rather stable conditions in the preindustrial period (Figure 1b). Long-term trends and year-to-year variations are very similar between the two regions. While during the first 100 years

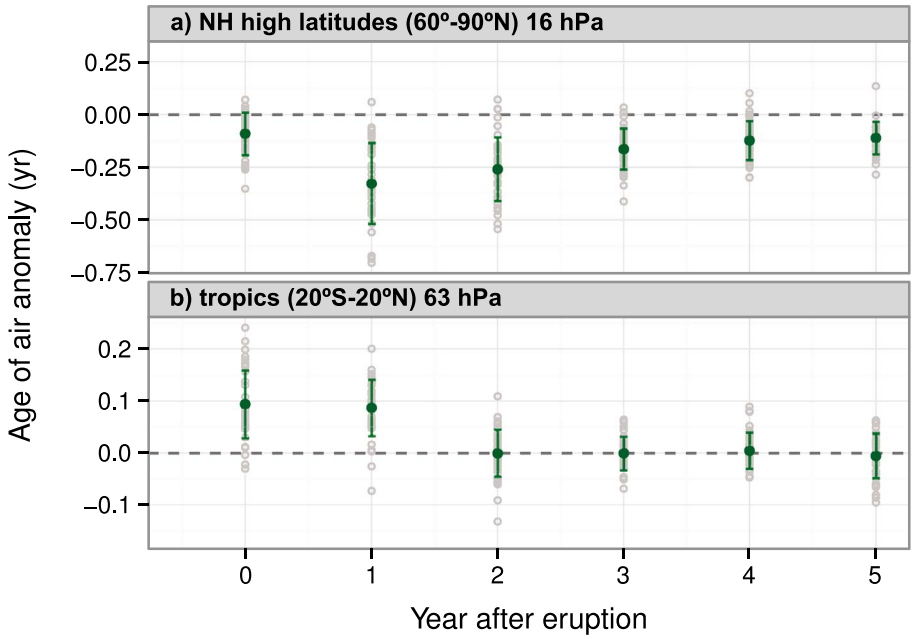

Figure 2. AoA composite for (a) the middle stratosphere of the NH high latitudes and (b) the tropical lower stratosphere averaged over the 10 strongest volcanic eruptions of the period 1620 to 2100 (see text and supporting information for details). The average overall eruptions and experiments is shown by the green dots with the bars indicating the ensemble standard deviation. Thin gray circles represent the individual simulations and eruptions.

of the simulations, until around 1700, a slight AoA increase is found, no pronounced long-term changes are visible until the beginning of the twentieth century. Nevertheless, year-to-year variations and a clear imprint of strong volcanic eruptions on AoA are simulated in the preindustrial era.

In the twentieth century, a negative AoA trend develops and continues until the middle of the 21st century (Figure 1b) with the largest changes occurring during the last three decades of the twentieth century. Several previous studies have attributed these changes to rising concentrations of GHGs, with increasing temperatures in the troposphere and cooling in the stratosphere, and the stratospheric temperature changes related to the ozone-depleting effect caused by different ODS [*Austin et al.*, 2007; *Li et al.*, 2008; *Oberländer-Hayn et al.*, 2015]. Future changes consequently depend on the emission scenario applied. The RCP 4.5, with a stabilization of the GHG emission toward the middle of the 21st century and a continuous reduction of ODS, leads to a slowdown of the global mean surface temperature rise from 2060 onward and an ongoing recovery of stratospheric ozone [*Anet et al.*, 2013a]. This climatic change is reflected in the stabilization of AoA trends in the second half of the 21st century.

3.1. Short-Term Variations: Volcanic Signals

In the preindustrial period, strong volcanic eruptions cause the largest changes in AoA on a time scale of several years. A superposed epoch analysis over the 10 strongest volcanic eruptions of the period 1620 to 2100 in the four simulations is performed to detect the characteristics of the AoA response (detailed method description in the supporting information). With the start of the eruption, positive AoA anomalies are found in the lower stratosphere and reduced values in the middle and upper stratosphere without any pronounced differences between the hemispheres (Figure S1a). The strongest negative anomalies during the first year of the eruption occur in the tropics. In the second year, AoA anomalies are almost equally distributed along the latitudes, while the recovery to background conditions starts in the third year in the tropical latitudes (Figures S1b and S1c). The analysis for the two AoA regions defined above reveals a consistent response for almost all eruptions with reduced ages in the tropical lower stratosphere and increased ages in the middle stratosphere of the NH high latitudes (Figure 2). The reduction in the NH high latitudes is significant, and the anomaly reaches its largest reduction of −8.4% in the second year. This AoA reduction is related to enhanced wave activity after the eruption (Figure S2). Especially the stratosphere of the northern midlatitudes to high latitudes shows an increase in vertical wave propagation connected with a convergence of the Eliasen-Palm flux and enhanced wave drag. This wave drag strengthens the poleward transport of air with rising motion

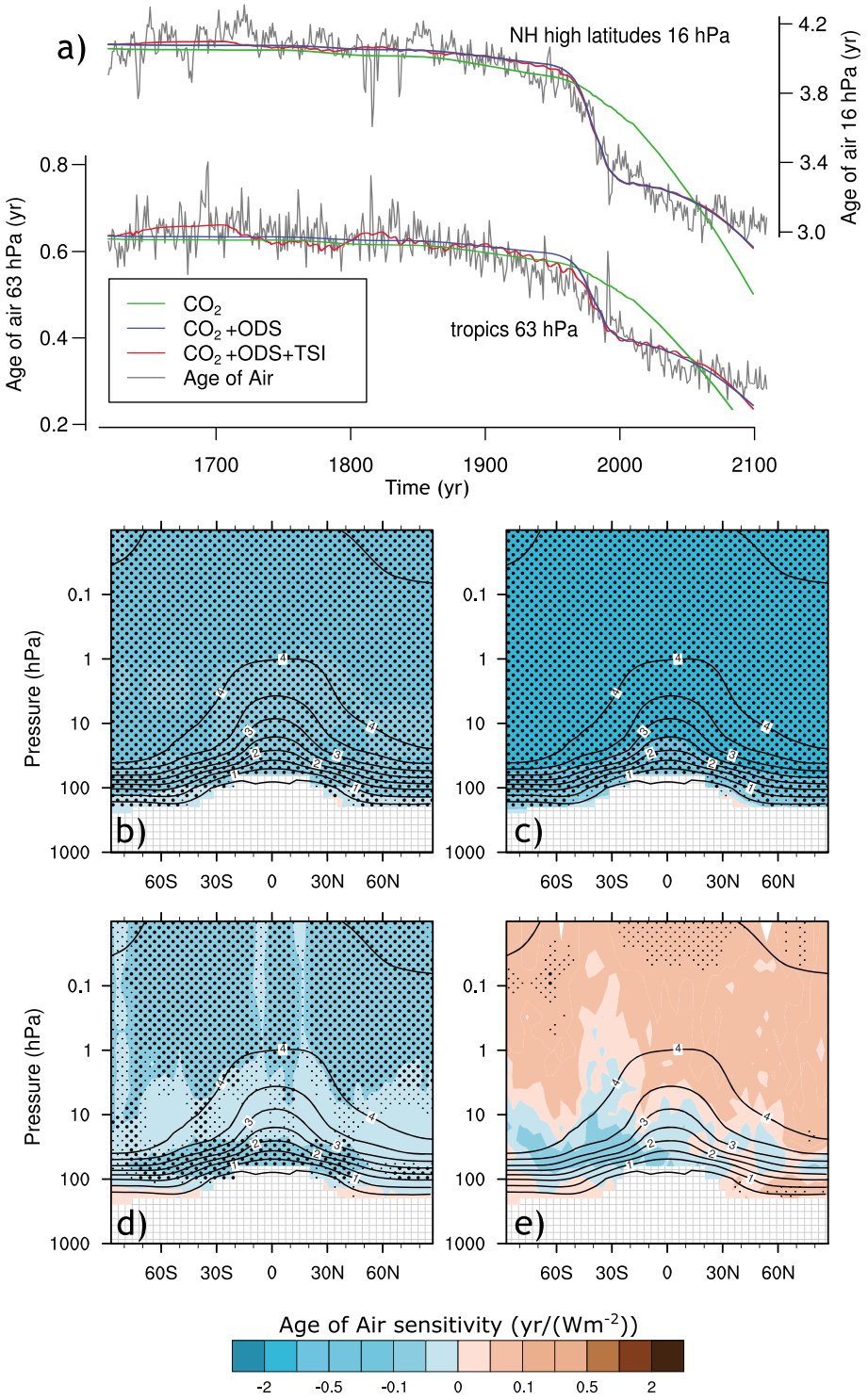

Figure 3. Regression coefficients of a multiple linear regression analysis between the radiative forcings of CO_2, ODS, TSI and AoA. (a) Stepwise regression between the AoA in the middle stratosphere of the NH high latitudes and the tropical lower stratosphere against different combinations of external radiative forcings. (b–d) Multiple linear regression coefficients over the period 1620–2100 for CO_2 (Figure 3b), ODS (Figure 3c), and TSI (Figure 3d). To allow for a comparison, we calculated the radiative forcing for each forcing factor (following *Ramaswamy et al.* [2001] for CO_2 and CFC-11. The TSI was scaled to the surface of the Earth assuming a reduction of 78% through absorption and stratospheric adjustment [*Gray et al.*, 2009]). (e) TSI coefficient for the two future simulations with 11year cycle solar variability only (CONST). Stippling indicates significant regression coefficients (thick stippling: $p \leq 0.05$, smaller stippling $p \leq 0.1$). Gray contours denote the climatological annual mean AoA during the preindustrial period.

in the tropics and downward motion in the high latitudes [*Andrews et al.*, 1987]. In the tropical lower stratosphere, AoA increases, but the anomalies are larger and the spread among the eruptions and simulations is larger (Figure 2). The largest response of AoA (+16.9%) is found in the first year after the eruption. Furthermore, the positive anomaly lasts only for about 2 years after the eruption. The opposing response in AoA between the lower and the middle stratosphere is found in the tropical upward mass flux as well. At 100 hPa, negative anomalies of −7% are found in the first and second years after the eruption, while at 25 hPa the mass flux increases by 17% (Figure S3). Additionally, the different responses of the lower and middle stratosphere can be seen in the transformed Eulerian mean (TEM) mass stream function (Figure S4). Here the weakening of the circulation in the lower stratosphere is directly connected to a weakening in the troposphere. At higher levels the TEM mass stream function is enhanced in both hemispheres. The reduction in the lower stratosphere can be related to a reduced exchange between troposphere and stratosphere, for instance, due to a weakening of strong tropical convection as a consequence of surface cooling after the eruption. Furthermore, the increased stability in the lower tropical stratosphere due to the aerosol warming reduces the penetration of deep convection into the stratosphere. After 2 years, the aerosol concentration decreases and the stratospheric and tropospheric temperatures return to unperturbed states. The downwelling and mixing of air masses with reduced ages at higher latitudes then leads to negative AoA anomalies also in the lower stratosphere (Figure S1c).

3.2. Long-Term Variations: Contributions From CO_2, ODS, and Solar Forcing

The relative contributions of CO_2, ODS (with the combined forcing of CFC-11 and CFC-12), and TSI on AoA variations are quantified by a multilinear regression analysis. In a first step, the influence of volcanic aerosols on AoA is removed based on the results from the superposed epoch analysis (supporting information). The regression analysis is limited to the two simulations driven by the STRONG solar forcing. Using the ensemble mean of all four simulations leads to very similar results.

A stepwise regression was performed for both AoA regions (Figure 3a). To compare the contributions of the different forcing factors, we use the radiative forcing of CO_2, ODS (calculated following *Ramaswamy et al.* [2001]), and TSI (taking albedo and stratospheric adjustment into account [*Gray et al.*, 2009]) in the regression analysis. To a large extent, the continuous reduction of AoA starting about 1900 is dominated by the CO_2 changes (explained variance $R^2 = 0.84$ for the NH high latitudes and 0.82 for the tropical region). Including the effect of the ODS improves the regression ($R^2 = 0.94$ and 0.89 for the NH high latitudes and the tropics, respectively). In particular, the pronounced AoA trend in the late twentieth century can only be explained with the effect of the ODS. Furthermore, the model reveals that stratospheric ozone recovery due to a decline in ODS is the main driver for the weakening of the negative AoA trends in the middle of the 21st century supported by the reduced CO_2 increase in the RCP 4.5. Considering the solar forcing does not lead to a further improvement of the regression model in the middle stratosphere of the NH high latitudes ($R^2 = 0.94$). In the tropical lower stratosphere, a weak solar signal is detected ($R^2 = 0.90$).

The spatial patterns of the multiple linear regression for the different forcing factors are shown in Figures 3b–3d. CO_2 and ODS (Figures 3b and 3c) cause a clear reduction in AoA, which is present over the entire stratosphere and mesosphere. With a mean (strongest) response of −1.1 yr/(W m^{-2}) (−1.6 yr/(W m^{-2})) the influence of ODS is much larger than the CO_2 influence of −0.2 yr/(W m^{-2}) (−0.3 yr/(W m^{-2})). The concentrations of CFC-11 and CFC-12 in the atmosphere, however, are very small, and consequently their radiative forcing is much smaller than the radiative forcing of CO_2 (compare Figure 1). The net AoA change for CO_2 is therefore much larger than the change related to ODS. The correlation coefficients between CO_2 and AoA are close to −1 for all levels and latitudes above 70 hPa, while the ODS reach correlation coefficients between −0.5 and −0.7 (not shown).

TSI changes in the long-term experiments induce a significant reduction in AoA throughout the stratosphere with mean regression coefficients of −0.05 yr/(W m^{-2}) and the strongest response reaching −0.11 yr/(W m^{-2}) (Figure 3d). This response is dominated by pronounced multidecadal variations in the solar forcing reconstruction of *Shapiro et al.* [2011]. Without multidecadal solar variability the response to the solar forcing is different: Applying the regression analysis to the two future simulations, with 11 year cycle variations only (i.e., CONST), a positive relationship is detected, although the significance is low and limited mainly to the higher stratosphere (Figure 3e). The imprint of CO_2 and ODS on AoA is comparable between the future simulations and the long-term experiments (not shown).

Table 1. Change in AoA During the Middle of the Dalton Minimum (1805–1815) in the Ensemble Experiment Forced by UV Variations Only (UV) or by Variations in the Visible and Near-Infrared (non-UV) for the Middle Stratosphere of the NH High Latitudes (16 hPa, 60°N–90°N) and the Tropical Lower Stratosphere (63 hPa, 20°S–20°N)[a]

Region	Forcing	ΔAoA (Year)	ΔAoA (%)	*p* Value
NH high latitudes, middle stratosphere	non-UV	0.06	1.58	<0.01
NH high latitudes, middle stratosphere	UV	0.00	−0.07	0.89
Tropics, lower stratosphere	non-UV	0.02	3.59	0.05
Tropics, lower stratosphere	UV	−0.01	−2.30	0.15

[a]Significant differences to the ensemble of control simulations were tested by a Student's *t* test (*p* value).

Additionally, we assess how variations in different solar spectral intervals (UV versus non-UV) affect AoA for one grand solar minimum. The Dalton Minimum in the early nineteenth century is characterized by a TSI reduction of −4.9 W m^{-2} (non-UV: −4.7 W m^{-2}; UV: −0.2 W m^{-2}), when the difference is calculated for the middle of the Dalton Minimum (1805–1815) to the reference year 1780. In these simulations, a significant AoA increase is found in the middle of the Dalton Minimum in response to the reduced incoming non-UV short-wave radiation (Table 1). Note that this response is in agreement with the relationship found in the long-term experiments, where an increase in the solar forcing leads to a reduction in AoA. In the middle stratosphere of the NH high latitudes, the global mean AoA increases significantly by 1.6% and in the lower tropical stratosphere by 3.6%. Driving the model with UV variations only leads to a small reduction in AoA in both regions (−0.1 and −2.3%). These anomalies are found to be significant only in a few regions of the stratosphere in the Southern Hemisphere (Figure S6) but nevertheless suggest that the weak positive relationship between solar variation and AoA found for the 11 year cycle may be dominated by the UV effect. Non-UV changes, however, anticorrelate with AoA. This spectral interval may be dominant for the solar influence on AoA found on longer time scales and can be described as bottom-up effect since non-UV variations are most effective at the surface and affect the stratosphere from below. Their influence is significant at all latitudes and levels (Figure S6).

The results of the solar forcing therefore depend on the spectral interval considered. The response to the 11 year cycle is similar to the effect of the UV changes, while the response found for the long-term experiments, where multidecadal TSI variations dominate, is comparable to the response found for non-UV variations. Separating the analysis into a preindustrial and a modern period leads to very similar results for all forcings, besides the fact that ODS were not present during preindustrial times (Figure S7).

4. Discussion and Conclusions

The response of stratospheric AoA to both natural and anthropogenic forcings is detected in different ensembles of simulations for the period 1600 to 2100. With a series of continuous model simulations for 500 years, covering three grand solar minima and several strong volcanic eruptions, this study considerably extends the understanding of AoA variations on longer time scales.

The largest simulated changes during the twentieth century, driven by the anthropogenic emission of CO_2 and ODS, cause a reduction in AoA, which is in agreement with previous model studies [*Austin et al.*, 2007; *Li et al.*, 2008; *Oberländer-Hayn et al.*, 2015].

The stratospheric AoA change in the future depends on the emission scenario. With the RCP 4.5 applied in this study, a stabilization of AoA is expected in the middle of the 21st century but at substantially lower values than during the preindustrial period. The recovery of the stratospheric ozone concentrations strongly contribute to this stabilization.

In the preindustrial period, AoA variability is much smaller and no long-term changes are found. Volcanic eruptions are the main driver of variability on time scales of several years, reducing AoA in the middle and upper stratosphere and increasing AoA in the lower stratosphere. These results are consistent with previous modeling studies [*Pitari*, 1993; *Pitari and Mancini*, 2002; *Garcia et al.*, 2011; *Aquila et al.*, 2013; *Toohey et al.*, 2014] and studies based on observations of recent eruptions [*Graf et al.*, 2007; *Schnadt Poberaj et al.*, 2011; *Abalos et al.*, 2015]. *Diallo et al.* [2012] reported an AoA increase after Pinatubo, which they interpreted as a reduction of the tropopause crossings and a slowdown of the BDC. In our study, this AoA increase is limited to the lower stratosphere, while at higher levels the intensification of the BDC dominates.

In this study, a spectral solar forcing reconstruction with pronounced multidecadal variations has been applied. Still, the solar influence on AoA is weak and characterized by a negative correlation between the solar forcing and AoA, which is dominated by variations in the non-UV spectral interval. This negative relationship between solar variations and AoA is in disagreement with the proposed weakening of the BDC (increase in AoA) during phases with high solar activity [*Kodera and Kuroda*, 2002]. *Kodera and Kuroda* [2002], however, focused on the 11 year cycle variability, which is too small (~1 W m^{-2}) and too short to have a direct effect on tropospheric temperatures [*Beer et al.*, 2000; *Frame and Gray*, 2010] but strong enough to change stratospheric temperatures through changes in the UV radiation. A response in agreement with *Kodera and Kuroda* [2002] is found, when sensitivity simulations forced only by UV variations or experiments without long-term TSI changes (but an 11 year solar cycle) are considered. This response, however, is very weak and hardly significant. On multidecadal time scales the pronounced TSI variations have the potential to cause substantial changes in tropospheric temperatures [*Beer et al.*, 2000; *Ammann et al.*, 2007; *Anet et al.*, 2014]. These tropospheric changes counteract the stratospheric changes in AoA (implied by UV).

On millenial and orbital time scales, the cumulative effect of a change in the incoming solar radiation may lead to a stronger response of the AoA. Similarly, CO_2 or tropospheric temperature changes on millennial time scales may also affect the stratospheric circulation and the residence time of air in the stratosphere. Time slice experiments with CCMs would be one possible way to address this issue in follow-up studies.

Acknowledgments
We acknowledge constructive and detailed comments by two anonymous reviewers. This work has been supported by the Swiss National Science Foundation under grant CRSII2-147659 (FUPSOL II) and by the Competence Center Environment and Sustainability (CCES) under the project MAIOLICA-2. All simulations described in this study are archived at the University of Bern and are available on request.

References

Abalos, M., B. Legras, F. Ploeger, and W. J. Randel (2015), Evaluating the advective Brewer-Dobson circulation in three reanalyses for the period 1979–2012, *J. Geophys. Res. Atmos.*, *120*, 7534–7554, doi:10.1002/2015JD023182.

Ammann, C. M., F. Joos, D. S. Schimel, B. L. Otto-Bliesner, and R. A. Tomas (2007), Solar influence on climate during the past millennium: Results from transient simulations with the NCAR Climate System Model, *Proc. Natl. Acad. Sci.*, *104*, 3713–3718.

Andrews, D. G., J. R. Holton, and C. B. Leovy (1987), *Middle Atmosphere Dynamics*, 489 pp., Academic Press, Orlando, Fla.

Anet, J. G., et al. (2013a), Impact of a potential 21st century "grand solar minimum" on surface temperatures and stratospheric ozone, *Geophys. Res. Lett.*, *40*, 4420–4425, doi:10.1002/grl.50806.

Anet, J. G., et al. (2013b), Forcing of stratospheric chemistry and dynamics during the Dalton Minimum, *Atmos. Chem. Phys.*, *13*, 10,951–10,967, doi:10.5194/acp-13-10951-2013.

Anet, J. G., et al. (2014), Impact of solar versus volcanic activity variations on tropospheric temperatures and precipitation during the Dalton Minimum, *Clim. Past*, *10*, 921–938.

Aquila, V., L. D. Oman, R. Stolarski, A. R. Douglass, and P. A. Newman (2013), The response of ozone and nitrogen dioxide to the eruption of Mt. Pinatubo at southern and northern midlatitudes, *J. Atmos. Sci.*, *70*, 894–900, doi:10.1175/JAS-D-12-0143.1.

Arfeuille, F., D. Weisenstein, H. Mack, E. Rozanov, T. Peter, and S. Brönnimann (2014), Volcanic forcing for climate modeling: A new microphysics-based data set covering years 1600–present, *Clim. Past*, *10*, 359–375, doi:10.5194/cp-10-359-2014.

Austin, J., and F. Li (2006), On the relationship between the strength of the Brewer-Dobson circulation and the age of stratospheric air, *Geophys. Res. Lett.*, *33*, L17807, doi:10.1029/2006GL026867.

Austin, J., J. Wilson, F. Li, and H. Vömel (2007), Evolution of water vapor concentrations and stratospheric age of air in coupled chemistry-climate model simulations, *J. Atmos. Sci.*, *64*, 905–921, doi:10.1175/JAS3866.1.

Austin, J., L. W. Horowitz, M. D. Schwarzkopf, R. J. Wilson, and H. Levy (2013), Stratospheric ozone and temperature simulated from the preindustrial era to the present day, *J. Clim.*, *26*, 3528–3543, doi:10.1175/JCLI-D-12-00162.1.

Beer, J., W. Mende, and R. Stellmacher (2000), The role of the Sun in climate forcing, *Quat. Sci. Rev.*, *19*, 403–415, doi:10.1016/S0277-3791(99)00072-4.

Brönnimann, S., J. L. Annis, C. Vogler, and P. D. Jones (2007), Reconstructing the Quasi-Biennial Oscillation back to the early 1900s, *Geophys. Res. Lett.*, *34*, L22805, doi:10.1029/2007GL031354.

Bunzel, F., and H. Schmidt (2013), The Brewer-Dobson circulation in a changing climate: Impact of the model configuration, *J. Atmos. Sci.*, *70*, 1437–1455, doi:10.1175/JAS-D-12-0215.1.

Butchart, N. (2014), The Brewer-Dobson circulation, *Rev. Geophys.*, *52*, 157–184, doi:10.1002/2013RG000448.

Butchart, N., and A. A. Scaife (2001), Removal of chlorofluorocarbons by increased mass exchange between the stratosphere and troposphere, *Nature*, *410*, 799–802.

Butchart, N., et al. (2006), Simulations of anthropogenic change in the strength of the Brewer–Dobson circulation, *Clim. Dyn.*, *27*, 727–741, doi:10.1007/s00382-006-0162-4.

Butchart, N., et al. (2010), Chemistry-climate model simulations of twenty-first century stratospheric climate and circulation changes, *J. Clim.*, *23*, 5349–5374, doi:10.1175/2010JCLI3404.1.

Diallo, M., B. Legras, and A. Chédin (2012), Age of stratospheric air in the ERA-Interim, *Atmos. Chem. Phys.*, *12*, 12,133–12,154, doi:10.5194/acp-12-12133-2012.

Egorova, T., E. Rozanov, V. Zubov, and I. L. Karol (2003), Model for Investigating Ozone Trends (MEZON), *Izv. Atmos. Oceanic Phys.*, *39*, 277–292.

Engel, A., et al. (2009), Age of stratospheric air unchanged within uncertainties over the past 30 years, *Nat. Geosci.*, *2*, 28–31, doi:10.1038/ngeo388.

Frame, T. H. A., and L. J. Gray (2010), The 11-yr solar cycle in ERA-40 data: An update to 2008, *J. Clim.*, *23*, 2213–2222, doi:10.1175/2009JCLI3150.1.

Fu, Q., P. Lin, S. Solomon, and D. L. Hartmann (2015), Observational evidence of strengthening of the Brewer-Dobson circulation since 1980, *J. Geophys. Res. Atmos.*, *120*, 10,214–10,228, doi:10.1002/2015JD023657.

Garcia, R. R., and W. J. Randel (2008), Acceleration of the Brewer-Dobson circulation due to increases in greenhouse gases, *J. Atmos. Sci.*, *65*, 2731–2739, doi:10.1175/2008JAS2712.1.

Garcia, R. R., W. J. Randel, and D. E. Kinnison (2011), On the determination of age of air trends from atmospheric trace species, *J. Atmos. Sci.*, *68*, 139–154, doi:10.1175/2010JAS3527.1.

Garny, H., T. Birner, H. Bönisch, and F. Bunzel (2014), The effects of mixing on age of air, *J. Geophys. Res. Atmos.*, *119*, 7015–7034, doi:10.1002/2013JD021417.

Giorgetta, M. A., L. Bengtsson, and K. Arpe (1999), An investigation of QBO signals in the east Asian and Indian monsoon in GCM experiments, *Clim. Dyn.*, *15*, 435–450, doi:10.1007/s003820050292.

Graf, H.-F., Q. Li, and M. A. Giorgetta (2007), Volcanic effects on climate: Revisiting the mechanisms, *Atmos. Chem. Phys.*, *7*, 4503–4511, doi:10.5194/acp-7-4503-2007.

Gray, L. J., S. T. Rumbold, and K. P. Shine (2009), Stratospheric temperature and radiative forcing response to 11-year solar cycle changes in irradiance and ozone, *J. Atmos. Sci.*, *66*, 2402–2417, doi:10.1175/2009JAS2866.1.

Hall, T. M., and R. A. Plumb (1994), Age as a diagnostic of stratospheric transport, *J. Geophys. Res.*, *99*, 1059–1070, doi:10.1029/93JD03192.

Holton, J. R., P. H. Haynes, M. E. McIntyre, A. R. Douglass, R. B. Rood, and L. Pfister (1995), Stratosphere-troposphere exchange, *Rev. Geophys.*, *33*, 403–439.

Kodera, K., and Y. Kuroda (2002), Dynamical response to the solar cycle, *J. Geophys. Res.*, *107*, 4749, doi:10.1029/2002JD002224.

Li, F., J. Austin, and J. Wilson (2008), The strength of the Brewer-Dobson circulation in a changing climate: Coupled chemistry-climate model simulations, *J. Clim.*, *21*, 40–57, doi:10.1175/2007JCLI1663.1.

Marsland, S. (2003), The Max-Planck-Institute global ocean/sea ice model with orthogonal curvilinear coordinates, *Ocean Model.*, *5*, 91–127, doi:10.1016/S1463-5003(02)00015-X.

Muthers, S., et al. (2014), The coupled atmosphere-chemistry-ocean model SOCOL-MPIOM, *Geosci. Model Dev.*, *7*, 2157–2179, doi:10.5194/gmd-7-2157-2014.

Oberländer, S., U. Langematz, and S. Meul (2013), Unraveling impact factors for future changes in the Brewer-Dobson circulation, *J. Geophys. Res. Atmos.*, *118*, 10,296–10,312, doi:10.1002/jgrd.50775.

Oberländer-Hayn, S., S. Meul, U. Langematz, J. Abalichin, and F. Haenel (2015), A chemistry-climate model study of past changes in the Brewer-Dobson circulation, *J. Geophys. Res. Atmos.*, *120*, 6742–6757, doi:10.1002/2014JD022843.

Pitari, G. (1993), A numerical study of the possible perturbation of stratospheric dynamics due to Pinatubo aerosols: Implications for tracer transport, *J. Atmos. Sci.*, *50*, 2443–2461, doi:10.1175/1520-0469(1993)050<2443:ANSOTP>2.0.CO;2.

Pitari, G., and E. Mancini (2002), Short-term climatic impact of the 1991 volcanic eruption of Mt. Pinatubo and effects on atmospheric tracers, *Nat. Hazards Earth Syst. Sci.*, *2*, 91–108, doi:10.5194/nhess-2-91-2002.

Ploeger, F., M. Riese, F. Haenel, P. Konopka, R. Müller, and G. Stiller (2014), Variability of stratospheric mean age of air and of the local effects of residual circulation and eddy mixing, *J. Geophys. Res. Atmos.*, *120*, 716–733, doi:10.1002/2014JD022468.

Ploeger, F., M. Abalos, T. Birner, P. Konopka, B. Legras, R. Müller, and M. Riese (2015), Quantifying the effects of mixing and residual circulation on trends of stratospheric mean age of air, *Geophys. Res. Lett.*, *42*, 2047–2054, doi:10.1002/2014GL062927.

Plumb, R. A. (2002), Stratospheric transport, *J. Meteorol. Soc. Jpn.*, *80*, 793–809, doi:10.2151/jmsj.80.793.

Ramaswamy, V., O. Boucher, J. Haigh, D. Hauglustine, J. Haywood, G. Myhre, T. Nakajima, G. Y. Shi, and S. | Solomon (2001), Radiative forcing of climate change, in *IPCC Third Assessment Report: Climate Change 2001*, edited by J. Houghton et al., chap. 6, pp. 350–416, Cambridge Univ. Press, Cambridge, U. K., and New York.

Remsberg, E. E. (2015), Methane as a diagnostic tracer of changes in the Brewer-Dobson circulation of the stratosphere, *Atmos. Chem. Phys.*, *15*, 3739–3754, doi:10.5194/acp-15-3739-2015.

Röckmann, T., J. Kaiser, C. A. M. Brenninkmeijer, J. N. Crowley, R. Borchers, W. A. Brand, and P. J. Crutzen (2001), Isotopic enrichment of nitrous oxide ($^{15}N^{14}NO$, $^{14}N^{15}NO$, $^{14}N^{14}N^{18}O$) in the stratosphere and in the laboratory, *J. Geophys. Res.*, *106*, 10,403–10,410, doi:10.1029/2000JD900822.

Roeckner, E., et al. (2003), The atmospheric general circulation model ECHAM5—Model description, *MPI Rep.*, Max-Planck Institute for Meteorology, Hamburg, Germany.

Rozanov, E., M. E. Schlesinger, V. Zubov, F. Yang, and N. G. Andronova (1999), The UIUC three-dimensional stratospheric chemical transport model: Description and evaluation of the simulated source gases and ozone, *J. Geophys. Res.*, *104*, 11,755–11,781, doi:10.1029/1999JD900138.

Schnadt Poberaj, C., J. Staehelin, and D. Brunner (2011), Missing stratospheric ozone decrease at Southern Hemisphere middle latitudes after Mt. Pinatubo: A dynamical perspective, *J. Atmos. Sci.*, *68*, 1922–1945, doi:10.1175/JAS-D-10-05004.1.

Shapiro, A. I., W. Schmutz, E. Rozanov, M. Schoell, M. Haberreiter, A. V. Shapiro, and S. Nyeki (2011), A new approach to the long-term reconstruction of the solar irradiance leads to large historical solar forcing, *Astron. Astrophys.*, *529*, A67, doi:10.1051/0004-6361/201016173.

Shepherd, T. G., and A. I. Jonsson (2008), On the attribution of stratospheric ozone and temperature changes to changes in ozone-depleting substances and well-mixed greenhouse gases, *Atmos. Chem. Phys.*, *8*, 1435–1444, doi:10.5194/acp-8-1435-2008.

SPARC (2010), SPARC CCMVal Report on the Evaluation of Chemistry-Climate Models, edited by V. Eyring, T. Shepherd and D. Waugh, SPARC Rep., 5, WCRP-30/2010, WMO/TD-40. [Available at www.sparc-climate.org/publications/sparc-reports/.]

Stenke, A., M. Schraner, E. Rozanov, T. Egorova, B. Luo, and T. Peter (2013), The SOCOL version 3.0 chemistry-climate model: Description, evaluation, and implications from an advanced transport algorithm, *Geosci. Model Dev.*, *6*, 1407–1427, doi:10.5194/gmd-6-1407-2013.

Stiller, G. P., et al. (2008), Global distribution of mean age of stratospheric air from MIPAS SF_6 measurements, *Atmos. Chem. Phys.*, *8*, 677–695, doi:10.5194/acp-8-677-2008.

Toohey, M., K. Krüger, M. Bittner, C. Timmreck, and H. Schmidt (2014), The impact of volcanic aerosol on the Northern Hemisphere stratospheric polar vortex: Mechanisms and sensitivity to forcing structure, *Atmos. Chem. Phys.*, *14*, 13,063–13,079, doi:10.5194/acp-14-13063-2014.

Waugh, D. (2009), The age of stratospheric air, *Nat. Geosci.*, *2*, 14–16.

Waugh, D. W., and T. M. Hall (2002), Age of stratospheric air: Theory, observations, and models, *Rev. Geophys.*, *40*(4), 1010, doi:10.1029/2000RG000101.